Chinese Chemical Letters 35 (2024) 108333

Contents lists available at ScienceDirect

Chinese Chemical Letters

journal homepage: www.elsevier.com/locate/cclet

Photoluminescent nickel(II) carbene complexes with ligand-to-ligand charge-transfer excited states

Chun-Liang Hou[a,b,1], Jia-Xi Song[a,b,1], Xiaoyong Chang[c], Yong Chen[a,b,*]

[a] Key Laboratory of Photochemical Conversion and Optoelectronic Materials & CAS-HKU Joint Laboratory on New Materials, Technical Institute of Physics and Chemistry, Chinese Academy of Sciences, Beijing 100190, China
[b] University of Chinese Academy of Sciences, Beijing 100049, China
[c] Department of Chemistry, Southern University of Science and Technology, Shenzhen 518055, China

ARTICLE INFO

Article history:
Received 8 January 2023
Revised 5 March 2023
Accepted 12 March 2023
Available online 15 March 2023

Keywords:
Nickel(II) complexes
N-Heterocyclic carbene
Luminescence
Ligand-to-ligand charge-transfer character
Low-lying d-d excited states

ABSTRACT

While nickel(II) complexes have been widely used as catalysts for carbon-carbon coupling reactions, the exploration of their photophysical and photochemical properties is still in the infancy. Here, a series of square-planar Ni(II) complexes [(diNHC)NiX_2] bearing chelating benzimidazole-based bis(*N*-heterocyclic carbene) ligands and varying anionic coligands (**1**, X = Cl; **2**, X = Br; **3**, X = I) are synthesized and structurally characterized. In solid state, both **1** and **2** exhibit orange-red photoluminescence under ambient conditions. The photophysical and electrochemical measurements along with density functional theory (DFT) calculations reveal that the low-energy emissions can be attributed to singlet excited states with ligand-to-ligand charge-transfer (LLCT) character. This work suggests that strong-field *N*-heterocyclic carbene ligands play a crucial role to achieve the luminescence of Ni(II) complexes.

Platinum(II) and palladium(II) complexes with d^8 valence electron configuration usually display efficient charge-transfer (CT) luminescence [1–11], which has been extensively used in optoelectronic devices [2,7,11–13], bio-imaging [2,14,15], photocatalytic reactions [16–20] and so on. However, their scarcity and high costs have stimulated the search for candidates based on earth-abundant elements [21,22]. Nickel, as a first-row transition metal that belongs to the same periodic group as palladium and platinum, provides an economically and ecologically benign alternative to precious metal systems [22]. However, photoluminescent nickel(II) complexes with charge-transfer excited state character are very rare [23–25]. The lack of luminescence properties of Ni(II) complexes can be attributed to their little metal-ligand orbitals overlap between the contracted $3d^8$ metal center orbitals and the relevant ligand orbitals, which leads to relatively weak d-d ligand-field (LF) splitting energies and low-lying d-d LF excited states [26]. As a result, these structurally distorted metal-centered (MC) LF states provide a thermally-activated d-d deactivation pathway for other close-lying excited states (*i.e.*, CT states) and thus quench the emission (Scheme 1a) [27,28].

Theoretically, the thermally-activated d-d deactivation process can be suppressed by increasing the energy gap (ΔE) between the CT and d-d states, which can be realized by either raising the d-d state or lowering the CT state. To this end, Yam and coworkers recently reported an emissive cyclometalated Ni(II) complex by introducing a pincer-type 1,3-di(pyridin-2-yl)benzene (N^C^N) ligand and a strong σ-donating carbazolyl ligand (Scheme 1b) [29]. In solid state, this complex was found to demonstrate weak luminescence at room temperature and intense luminescence at low temperature with excited state lifetimes in the submicrosecond regime. *N*-Heterocyclic carbene compounds (NHCs) are characterized by strong σ-donating ability, which have been used as ligands to synthesize photoluminescent transition metal complexes, *i.e.*, platinum(II) [30–33], iridium(III) [34–37] and gold(I) [38–45]. We envision that such strong σ-donor properties of NHCs are capable of pushing nonradiative MC d-d transitions to higher energy, thereby generating emissive Ni(II) complexes.

Herein, we designed, synthesized and structurally characterized a class of square-planar Ni(II) carbene complexes containing benzimidazole-based *N*-heterocyclic carbene ligands and halogen ligands (Scheme 1c). The [(diNHC)NiX_2] (X = Cl or Br) complexes show solid-state luminescence under ambient conditions with temperature-independent lifetimes. A combination of pho-

* Corresponding author at: Key Laboratory of Photochemical Conversion and Optoelectronic Materials & CAS-HKU Joint Laboratory on New Materials, Technical Institute of Physics and Chemistry, Chinese Academy of Sciences, Beijing 100190, China.
E-mail address: chenyong@mail.ipc.ac.cn (Y. Chen).
[1] These authors contributed equally to this work.

https://doi.org/10.1016/j.cclet.2023.108333
1001-8417/

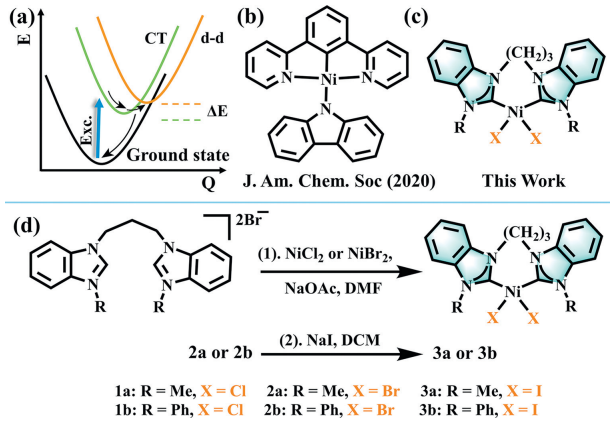

Scheme 1. (a) A thermally-activated deactivation pathway for Ni(II) complexes. Exc., excitation; CT, the emissive charge-transfer state; d-d, low-lying metal-centered excited states; black arrows represent vibrational relaxation and non-radiative decay. (b) Representative Ni(II) complex emitter. (c) Molecular structures of Ni(II) complexes in this work. (d) Synthetic routes of complexes **1**–**3a** and **1**–**3b**.

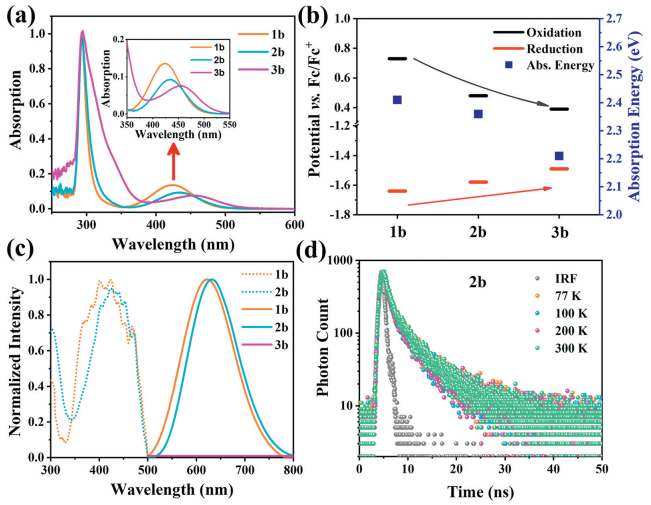

Fig. 2. (a) Absorption spectra of complexes **1**–**3b** in dichloromethane. (b) Electrochemical redox potentials and transition energies for CT states of **1**–**3b**. The energy of the CT state was estimated from the onset of the absorption band in dichloromethane, where the intensity was 0.10 at λ_{max}. (c) Normalized excitation and emission spectra of complexes **1**–**3b** in solid state at room temperature. (d) Normalized PL decay at different temperatures for complex **2b**.

tophysical properties and density functional theory (DFT) calculations unveils that the orange-red emission is derived from the S_1 state having predominant ligand (halogen)-to-ligand (NHCs) charge-transfer (LLCT) character.

The synthetic routes to Ni(II) carbene complexes are depicted in Scheme 1d and further experimental details are provided in the Supporting information. The synthesis of ligand precursors have been described previously [46–48]. Complexes [(diNHC)$NiCl_2$] and [(diNHC)$NiBr_2$] were readily prepared by stirring the corresponding ligands with nickel halide in dimethylformamide in the presence of NaOAc under reflux conditions. After reaction, the precipitate was filtered, washed by water and recrystallized from methanol to give yellow solid. [(diNHC)NiI_2] was obtained by simple ligand exchange [46]. All complexes have been characterized by ^{1}H nuclear magnetic resonance (NMR), ^{13}C NMR, and high-resolution ESI (HR-ESI) mass spectrometry and elemental analyses (Scheme S1, Figs. S1–S19 in Supporting information).

Dark yellow single crystals of **1**–**3b** were obtained by slow diffusion of hexane into saturated dichloromethane solutions at room temperature and their structures have been determined through single-crystal X-ray diffraction analysis. The selected bond lengths of Ni-C_{NHC} and Ni-X bonds and bond angles around the metal center are given in Tables S1 and S2 (Supporting information). As depicted in Fig. 1, all complexes have an approximately square-planar coordination geometry. The C_{NHC}-Ni-C_{NHC} bite angle of the three complexes are consistent throughout the series, being 86.46° for **1b**, 86.96° for **2b**, 89.94° for **3b**. The X-Ni-X bite angles lie in the range of 93°–94°. The Ni-C_{NHC} bonds in three complexes have an average bond length of 1.86 Å, which is shorter than the reported Ni(II) complexes [23,25,49], implying that the benzimidazole derived *N*-heterocyclic carbene ligands can serve as a strong σ-donor ligand to raise the energy of the MC excited state. Additionally, for halogen atoms with coplanar structures, the Ni-X bond length increases with increasing atomic radius of X, 2.23 Å for **1b**, 2.35 Å for **2b**, and 2.55 Å for **3b**. All Ni(II) complexes pair in a head-to-tail manner with intermolecular Ar-H···X and intramolecular Ar-H···X (2.8–3.2 Å) (Figs. S20–S22 in Supporting information).

The ultraviolet–visible (UV–vis) absorption spectra of Ni(II) complexes **1**–**3a** and **1**–**3b** were recorded at 298 K in diluted dichloromethane (Fig. 2a and Fig. S23 in Supporting information), and the photophysical data are collected in Table S3 (Supporting information). All Ni(II) complexes exhibit similar UV–vis absorption spectra with absorption maxima at 292 nm and a weak and broad absorption band between 350 and 550 nm, the latter accounting for the yellow color of Ni(II) complexes. The high energy absorption region of the Ni(II) complexes are the same as ligands **a** and **b** (Fig. S24 in Supporting information). The lowest-energy absorption band of all Ni(II) complexes exhibit slightly blue-shifted with increasing solvent polarity from dichloromethane to acetone to acetonitrile (Fig. S25 in Supporting information). Hence, the high energy absorption band is attributed to localized π-π^* transitions of the carbene moiety, while the lowest-energy absorption band in the visible range is ascribed to CT interactions between halogen units or nickel metal center and benzimidazole-based carbenes. As shown in Fig. 2a and Table S3, with the variation of anions (Cl, Br, I), the maximum absorption peaks of complexes **1**–**3b** undergo a red shift in dichloromethane from 424 nm to 456 nm. In addition, when the two phenyl substituents of benzimidazole carbenes are replaced by methyl groups, a blue shift of the absorption peak

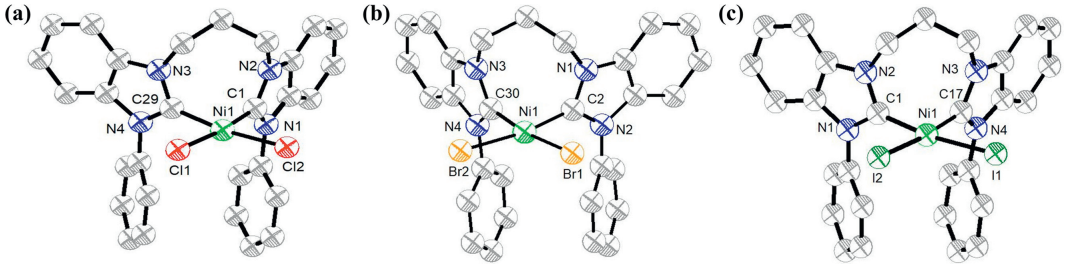

Fig. 1. Thermal ellipsoid plots of (a) **1b**, (b) **2b** and (c) **3b**.

is observed in dichloromethane. These spectral differences are attributed to the effect of halide anions and benzimidazole carbenes on the energy levels of the ground state frontier molecular orbitals (FMOs). These data suggest that the relatively low-energy bands can be assigned to a mixture of LLCT and d-d transitions (see theoretical calculations section).

The redox properties of **1**–**3a** and **1**–**3b** were determined using cyclic voltammetry (CV) and differential pulse voltammetry (DPV) in dry and degassed dimethylformamide solutions (0.1 mol/L nBu$_4$NPF$_6$) at room temperature. All potentials are referenced *vs*. ferrocene/ferrocenium (Fc/Fc$^+$) as internal standard which are listed in Table S4 (Supporting information) and graphically presented in Fig. 2b and Figs. S26 and S27 (Supporting information). The oxidation and reduction of all complexes exhibit irreversible waves, which may be caused by coordination of a solvent molecule and anionic ligand dissociation. Notably, the first reduction potentials of complexes **1**–**3b** gradually shift towards a more positive potential. Besides, the first oxidation potentials for **1**–**3b** are highly sensitive to the identity of anionic ligands. A pronounced cathodic shift in the oxidation potentials for **1**–**3b** is observed in the range Cl < Br < I, leading to a similar shift in the lowest-energy absorption band. The energy level of highest occupied molecular orbitals (HOMOs) is dominated by contribution from the halide orbitals. Furthermore, a slight shift to more negative potentials for the first reduction peaks along with a blue-shift in the lowest-energy absorption band, is observed for given complexes, *e.g.*, **1a** *versus* **1b**, **2a** *versus* **2b**, and **3a** *versus* **3b**. The oxidation and reduction potentials of all complexes are consistent with the CT transition of these complexes.

Although no detectable emission was observed for Ni(II) complexes in solution, the solid-state luminescence was clearly visible to the naked eye under 365 nm UV irradiation. Hence, photoluminescent properties of Ni(II) complexes were investigated in solid state at room temperature (Fig. 2c). The emission spectra ($\lambda_{max(em)} = 620$ nm for **1b**; $\lambda_{max(em)} = 631$ nm for **2b**; solid line) and excitation spectra ($\lambda_{max(ex)} = 410$ nm for **1b**; $\lambda_{max(ex)} = 425$ nm for **2b**; dotted line) of Ni(II) complexes were recorded. The designed Ni(II) complexes display large Stokes shifts with excitation and emission peaks, which are similar to that reported in previous literature [24]. When iodide ions act as anionic coligands, **3b** is found to be nonemissive at both low and ambient temperatures due to the iodine-induced heavy atom effect which enhanced intersystem crossing (ISC) and then quenched fluorescence [50].

Thermally activated delayed fluorescence (TADF) and room-temperature phosphorescence (RTP) emitters typically involve triplet excitons that are particularly sensitive to temperature and molecular oxygen [40,51,52]. The emission intensity and peak position of complexes **1**–**2b** are not perturbed by oxygen (Fig. S29 in Supporting information), which indicates no involvement of triplet state. The photoluminescence (PL) decays of complex **2b** at different temperatures (77–300 K) were determined by time-correlated single photon counting (TCSPC), whose emission is fluorescence with a temperature-independent lifetime of 3.01–3.12 ns (Fig. 2d). The PL lifetime curves are slightly longer than the temporal width of the IRF. The PL decays of complex **1b** show the same result at various temperatures (77–300 K) with lifetime of 1.61–1.89 ns (Fig. S31 in Supporting information). There is no evidence for either delayed fluorescence or phosphorescence in **1**–**2b**. As mentioned earlier, complexes **1**–**2b** display large Stokes shifts in solid state and electrochemical properties. We can confidently attribute the low-energy emission of **1**–**2b** to fluorescence from the excited singlet state.

To investigate the electronic structure features among complexes **1**–**3b**, DFT and time-dependent density functional theory (TDDFT) calculations are employed. The geometries, FMOs, corresponding energy levels and atoms/fragments distributions of three

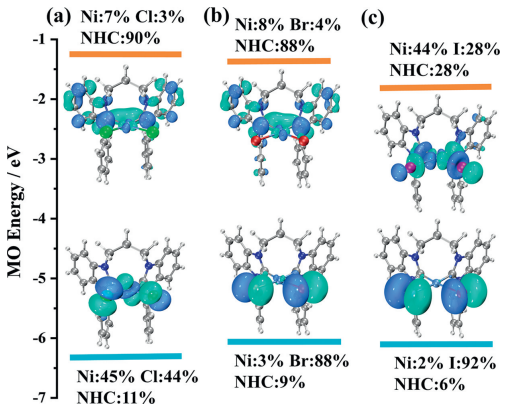

Fig. 3. Frontier molecular orbital isosurfaces and energies of (a) **1b**, (b) **2b**, and (c) **3b** in the solid S_0 states at the crystal S_0 geometries without the optimization of heavy atoms (isovalue = 0.04). The corresponding fragment distributions of each FMO are also illustrated.

complexes in solid state are displayed in Fig. 3 based on each crystal S_0 structure. Accompanied with the varying of halogen ligands, little structural difference but obvious gradation of FMO components and energies are formed. The HOMO of **1b** is mainly accorded by NiX_2 parts (Ni 45% + X_2 44%), while the HOMOs in **2b** (Ni 3% *vs*. X_2 88%) and **3b** (Ni 2% *vs*. X_2 92%) are lack of Ni participation. Similar but opposite trend resulting from the halogen donor ability is also observed in the analysis of the lowest unoccupied molecular orbitals (LUMOs). The LUMO of **1b** is mainly formed by NHC carbene unit with little Ni composition. However, when the halogen ligand switches to I, a Ni atom involvement cannot be ignored. The composition changing confirms the emissive phenomenon, as a lower composition of Ni in FMOs would improve the effective emission by precluding the d-d MC state and forming LLCT state, especially in complex **2b**.

The simulated absorption spectra by TDDFT of all three complexes are displayed and the fit between calculated and observed in the visible region is acceptable (Table S5 in Supporting information). The lowest energy absorption bands can be identified as $S_0 \rightarrow S_4$ transitions. To gain the intuitive features of compositions in these transitions, we perform the natural transition orbitals (NTO) analyses. As shown in Fig. S32 (Supporting information), all $S_0 \rightarrow S_4$ transitions get the obvious LLCT and d-d features. Since a low-lying d-d MC state is essential for photoluminescence quenching, we further study the role of LF splitting Ni d-orbitals in FMOs, especially highest occupied LF d_{z2} and lowest unoccupied LF d_{x2-y2}. As given in Fig. S33 (Supporting information), the features of Ni d_{z2} orbitals are performed in HOMO-1 for **1b** and HOMO-5 for **2b**/**3b**. Besides, the Ni d_{x2-y2} orbitals exhibit less significant in LUMO+3 for **1b**, LUMO+1 for **2b** and LUMO for **3b**. The larger d-d gaps shown in **1b** and **2b** imply that the decrease of d orbital compositions in FMOs means the less MC disturbance on LLCT state, so the photoluminescence would be lit up. Nonetheless, a widely dispersed Ni d orbital configuration in the LUMO of **3b** may offer the neighboring MC state, which might result in a thermally d-d deactivation pathway, which is consistent with our characterization that can quench the photoluminescence.

In summary, a class of square-planar nickel(II) carbene complexes bearing halogen ligands as electron donors have been prepared by a new synthetic route and structurally characterized by single-crystal X-ray diffraction. Wherein, the [(diNHC)NiX_2] (X = Cl or Br) complexes display apparent fluorescence with temperature-independent decay lifetimes in solid state. The experimental data and theoretical calculations altogether reveal that the solid-state fluorescence in Ni(II) complexes is likely to be a result of LLCT character. Collectively, these data lead us to conclude that NHCs are

demonstrated to be a sagacious choice in developing luminescent Ni(II) complexes in the red spectral region. Our study provides new ideas and strategies for Ni(II) complexes research in photophysics and photochemistry.

Declaration of competing interest

The authors declare that they have no known competing financial interests or personal relationships that could have appeared to influence the work reported in this paper.

Acknowledgments

This work is supported by the Natural Science Foundation of China (No. 22175191). Y.C. thanks the financial support from CAS-Croucher Funding Scheme for Joint Laboratories and Beijing Municipal Science & Technology Commission (No. Z211100007921020).

Supplementary materials

Supplementary material associated with this article can be found, in the online version, at doi:10.1016/j.cclet.2023.108333.

References

[1] M.H.Y. Chan, V.W.W. Yam, J. Am. Chem. Soc. 144 (2022) 22805–22825.
[2] K. Li, Y. Chen, J. Wang, C. Yang, Coord. Chem. Rev. 433 (2021) 213755.
[3] M.C. Tang, A.K.W. Chan, M.Y. Chan, V.W.W. Yam, Top. Curr. Chem. 374 (2016) 46.
[4] W.P. To, Q.Y. Wan, G.S.M. Tong, C.M. Che, Trends Chem. 2 (2020) 796–812.
[5] Q. Wan, J. Yang, W.P. To, C.M. Che, Proc. Natl. Acad. Sci. U. S. A. 118 (2021) e2019265118.
[6] Z.H. Wei, K. Zhang, C.K. Kim, et al., Chin. Chem. Lett. 32 (2021) 493–496.
[7] X.G. Wu, D.G. Chen, D.H. Liu, et al., J. Am. Chem. Soc. 142 (2020) 7469–7479.
[8] V.W.W. Yam, A.K.W. Chan, E.Y.H. Hong, Nat. Rev. Chem. 4 (2020) 528–541.
[9] B. Yang, G. Zou, S.L. Zhang, et al., Angew. Chem. Int. Ed. 60 (2021) 10531–10536.
[10] L. Yuan, Q.J. Ding, Z.L. Tu, et al., Chin. Chem. Lett. 33 (2022) 1459–1462.
[11] Y. Zhang, J. Miao, J. Xiong, K. Li, C. Yang, Angew. Chem. Int. Ed. 61 (2022) e202113718.
[12] A.K.W. Chan, M. Ng, Y.C. Wong, et al., J. Am. Chem. Soc. 139 (2017) 10750–10761.
[13] C. Wu, Y. Zhang, J. Miao, et al., Chin. Chem. Lett. 34 (2023) 107455.
[14] L.Z. Ma, T.F. Yang, Z.Y. Zhang, et al., Chin. Chem. Lett. 30 (2019) 1942–1946.
[15] X.Q. Zhou, M. Mytiliniou, J. Hilgendorf, et al., Adv. Mater. 33 (2021) 2008613.
[16] W.J. Choi, S. Choi, K. Ohkubo, et al., Chem. Sci. 6 (2015) 1454–1464.
[17] P. Domingo-Legarda, A. Casado-Sánchez, L. Marzo, et al., Inorg. Chem. 59 (2020) 13845–13857.
[18] F. Glaser, O.S. Wenger, Coord. Chem. Rev. 405 (2020) 213129.
[19] G.H. Wang, D. Peng, Y. Sun, C.L. Chen, CCS Chem. 3 (2021) 2025–2034.
[20] J.J. Zhong, W.P. To, Y. Liu, W. Lu, C.M. Che, Chem. Sci. 10 (2019) 4883–4889.
[21] S.Y. Lin, Q. Peng, Q. Ou, Z.G. Shuai, Inorg. Chem. 58 (2019) 14403–14409.
[22] O.S. Wenger, J. Am. Chem. Soc. 140 (2018) 13522–13533.
[23] J.D. Cope, J.A. Denny, R.W. Lamb, et al., J. Organomet. Chem. 845 (2017) 258–265.
[24] Y.M. Tian, X.N. Guo, I. Krummenacher, et al., J. Am. Chem. Soc. 142 (2020) 18231–18242.
[25] Y.H. Yao, G.L. Ran, C.L. Hou, et al., J. Am. Chem. Soc. 144 (2022) 7346–7356.
[26] C. Wegeberg, O.S. Wenger, JACS Au 1 (2021) 1860–1876.
[27] T. Ogawa, N. Sinha, B. Pfund, A. Prescimone, O.S. Wenger, J. Am. Chem. Soc. 144 (2022) 21948–21960.
[28] S.I. Ting, S. Garakyaraghi, C.M. Taliaferro, et al., J. Am. Chem. Soc. 142 (2020) 5800–5810.
[29] Y.S. Wong, M.C. Tang, M. Ng, V.W.W. Yam, J. Am. Chem. Soc. 142 (2020) 7638–7646.
[30] H. Amouri, Chem. Rev. 123 (2023) 230–270.
[31] X.C. Hang, T. Fleetham, E. Turner, J. Brooks, J. Li, Angew. Chem. Int. Ed. 52 (2013) 6753–6756.
[32] K. Li, G. Cheng, C. Ma, et al., Chem. Sci. 4 (2013) 2630–2644.
[33] K. Li, X. Guan, C.W. Ma, et al., Chem. Commun. 47 (2011) 9075–9077.
[34] J.Q. Han, Y.K. Chun, S.L. Chan, et al., CCS Chem. 4 (2022) 2354–2368.
[35] C. Wu, K.N. Tong, M. Zhang, et al., Adv. Opt. Mater. 10 (2022) 2200356.
[36] Y. Wu, C. Yang, J. Liu, et al., Chem. Sci. 12 (2021) 10165–10178.
[37] X.L. Yang, G.J. Zhou, W.Y. Wong, Chem. Soc. Rev. 44 (2015) 8484–8575.
[38] T.Y. Li, D.S.M. Ravinson, R. Haiges, P.I. Djurovich, M.E. Thompson, J. Am. Chem. Soc. 142 (2020) 6158–6172.
[39] Q. Liu, M. Xie, X.Y. Chang, et al., Angew. Chem. Int. Ed. 57 (2018) 6279–6283.
[40] A.S. Romanov, D. Di, L. Yang, et al., Chem. Commun. 52 (2016) 6379–6382.
[41] Y. Wang, J.P. Chang, R. Xu, et al., Chem. Soc. Rev. 50 (2021) 13559–13586.
[42] Y.S. Wang, L.Y. Sun, Y.Y. Wang, Y.F. Han, Sci. China Chem. 65 (2022) 1129–1133.
[43] J.G. Yang, K. Li, J. Wang, et al., Angew. Chem. Int. Ed. 59 (2020) 6915–6922.
[44] J.G. Yang, X.F. Song, G. Cheng, et al., ACS Appl. Mater. Interfaces 14 (2022) 13539–13549.
[45] Y.W. Zhang, S. Bai, Y.Y. Wang, Y.F. Han, J. Am. Chem. Soc. 142 (2020) 13614–13621.
[46] H.V. Huynh, C.H.M. Koh, V.H. Nguyen, Dalton Trans. 46 (2017) 11318–11326.
[47] M.H. Reineke, T.M. Porter, A.L. Ostericher, C.P. Kubiak, Organometallics 37 (2018) 448–453.
[48] H.V. Huynh, R. Jothibasu, Eur. J. Inorg. Chem. 2009 (2009) 1926–1931.
[49] A. Klein, B. Rausch, A. Kaiser, N. Vogt, A. Krest, J. Organomet. Chem. 774 (2014) 86–93.
[50] B.H. Farnum, W.M. Ward, G.J. Meyer, Inorg. Chem. 52 (2013) 840–847.
[51] Z. Wang, L. Gao, Y. Zheng, et al., Angew. Chem. Int. Ed. 61 (2022) e202203254.
[52] Z.H. Wang, Y. Zheng, Y. Su, et al., Sci. China Mater. 65 (2022) 2160–2168.